Evaluating the Co-Precessing Frame Approximation for Eccentric and Precessing Compact Binaries

Sam Johar, Taylor Knapp, Lucy Thomas
(Dated: July 10, 2025)

I. INTRODUCTION

Analysis of current LIGO data assumes that the orbit of a binary black hole (BH) system is quasi-circular. However, as detector sensitivity increases, we are more likely to begin observing eccentricity in detected waveforms. Part of the reason that LIGO detectors have not yet identified a non quasi-circular system is that eccentric binaries tend to circularize over time as gravitational waves emitted by the system radiate away eccentricity by removing excess angular momentum from the system. This circularizing effect can be seen in Figure 1, which depicts the inspiral of a low eccentricity waveform model. As detectors become more sensitive in the low frequency range (20Hz-50Hz), the inspirals of detected compact binary coalescences (CBCs) will be better resolved, giving us a better chance of seeing eccetricity before it has been radiated away. Additionally, now that we have identified many CBCs and analyzed them under the assumption of quasi-circularity, we are in a better position to relax this assumption going forward.

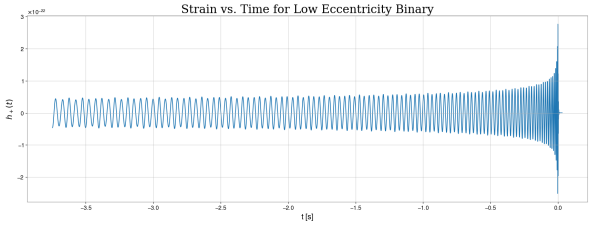

FIG. 1. Plus polarization of strain over time for the inspiral of a BH binary with 0.05 eccentricity. At the beginning of the inspiral, the periodic higher amplitude "knocking" characteristic of an eccentric system is clearly visible. One such knock can be seen just before the -3.5 second mark. However, these knocks become less clearly distinguishable throughout the inspiral. This waveform was generated with the LIGO Algorithm Library Simulation (LALSimulation) code package [1].

Binary black hole systems form in two main ways: isolated formation and dynamical capture. Isolated binaries are systems where the two bodies were orbiting each other in a binary before becoming black holes, while dynamical systems form when two pre-existing black holes approach each other, usually in a globular cluster, and are caught in each others' gravitational pull [2]. In isolated systems, we expect the orbit to be quasi-circular. However, we expect that dynamical systems could have eccentric orbits, in part because the binary will not have had as much time to radiate away eccentricity. Thus, detecting eccentric waveforms would provide evidence towards such systems being formed via dynamical capture. Modelling eccentricity allows researchers to stop making the assumption of quasi-circularity and will ensure that the tools exist to analyze eccentric waveforms when we eventually observe them.

Eccentricity (e) varies from 0 to 1 for bound systems, with e = 0 representing a circular orbit and e = 1 a parabolic orbit. In a quasi-circular orbit, each black hole has a constant angular velocity throughout one orbit. However when e > 0 and the orbit is elliptical, a black hole's angular velocity varies depending on the location in its orbit. At the point where the two black holes are closest together, known as **periastron**, the black holes travel with the fastest angular velocity and emit the highest amplitude GWs. Conversely, their angular velocity is slowest when they are farthest away from each other at **apastron**, and they emit lower amplitude GWs. These amplitude changes modulate the signal, creating periodic "knocks" at periastron[3]. Binaries with elliptical orbits will also experience **periastron precession**, an effect predicted by general relativity wherein an object's orbit itself precesses around the focus of its orbital ellipse within the orbital plane. This precession is due to ellipticity, and is not related to spin.

Taking into account the spins of the black holes in a CBC further complicates the observed GW. General relativity predicts that spinning objects affect the curvature of spacetime by "dragging" the space around them[4]. In a binary black hole system, we denote the orbital angular momentum vector $\overrightarrow{L}$. This vector is by definition always perpendicular to the instantaneous plane of orbit. When the spins of the black holes are parallel or anti-parallel to $\overrightarrow{L}$, the system has **aligned spins** and both the spins and orbital angular momentum remain fixed in direction[5]. Systems with aligned spins have been well modelled and investigated[6].

However, if the spins are not aligned with $\overrightarrow{L}$, the system is complicated by a precession effect known as **Lense-Thirring Precession**, which has been observed in detector data. Due to general relativity, a spinning black hole will drag the space around it within the plane of orbit, affecting the the GWs it emits. This dragging effect creates spin-orbit and spin-spin couplings, leading both the orbital plane (and thus $\overrightarrow{L}$) and the spins of the black holes themselves to precess[4]. Precession leads to modulation of the signal's amplitude and frequency as the alignment of the incoming GW with respect to the detector changes with $\overrightarrow{L}$, an effect that is demonstrated by Figure 2. The phase of the precessing waveform is also

modulated, though this effect is more difficult to observe in the plot.

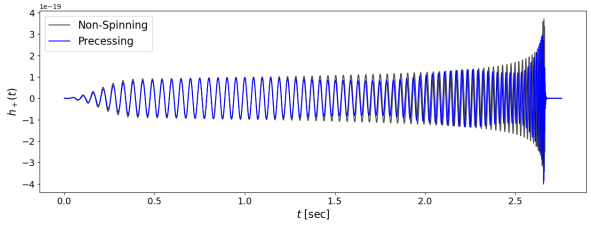

FIG. 2. Plus-polarization of strain over time for the inspiral of a precessing waveform (blue) and non-precessing waveform (grey). Amplitude modulation of the precessing waveform is clearly visible in contrast to the smooth amplitude increase in the non-precessing waveform. The two waveforms are roughly the same length, indicating that precession does not affect inspiral duration. Both waveforms were generated with LALSimulation [1].

The **co-precessing frame** is the reference frame that rotates with $\overrightarrow{L}$ such that $\overrightarrow{L}$ is always in the +z direction. Within the co-precessing frame, the complex seven-dimensional parameter space of a precessing system is reduced to a two-dimensional space built on waveforms that do not precess. One way to shift into this frame is to characterize the precessing system by describing $\overrightarrow{L}$'s position with respect to each axis with three time-dependent rotation angles, the most important of which is $\beta(t)$: the angle between $\overrightarrow{L}$ and the +z axis in the lab frame. Shifting into the co-precessing frame forces $\beta(t) = 0$, simplifying the system as described by Schmidt et al [6]. We utilize the minimal rotation condition version of the co-precessing frame, which enhances this technique by uniquely defining the rotation operator as described in Boyle et al. [7].

Inspiral-merger-ringdown (IMR) models for quasi-circular precessing systems are mature and have been used extensively for GW data analysis. IMR models with eccentric inspirals have also been used for data analysis more recently, but these models do not include eccentricity in the merger or ringdown phase—a fairly accurate approximation as a binary typically circularizes before the merger stage. Eccentric and precessing inspiral models using PN approximations exist, but no well-reviewed or tested eccentric and precessing IMR models exist as of yet. The closest current model [8], which is in early stages of development, has not yet been reviewed. This model uses the co-precessing frame approximation to construct eccentric and precessing IMR waveforms. However, while the co-precessing frame successfully counteracts precession effects for circular binaries, this "untwisting" effect has not been well studied for waveforms that are both eccentric and precessing.

II. OBJECTIVES

Our main objective is to study the effect of shifting to the co-precessing frame on eccentric and precessing waveforms. We hope to determine the accuracy of the co-precessing frame approximation in removing precession effects from eccentric waveforms, comparing the efficacy of this "untwisting" effect across three different waveform generation models. As the first two models are based on PN approximations, they are only accurate in the inspiral. Thus, we will specifically be studying this region of the CBC. If we find that some precession effects remain in "untwisted" waveforms, we will attempt to determine if they are systematic and thus follow a pattern which can be modelled, or if missing physics in the model means the approximation does not hold.

Determining a map from an eccentric and precessing waveform to an eccentric waveform through the co-precessing frame would make generating future more complicated models that go beyond **post-Newtonian** (PN) approximations easier. If we are able to determine a map between precessing and non-precessing waveforms, these future models could begin by creating non-precessing eccentric waveforms, then add in precession by "twisting" away from the co-precessing frame into an more complex eccentric and precessing waveform—an easier alternative to the complicated physics needed to model eccentric and precessing waveforms otherwise. A map into the co-precessing frame would additionally make it much easier to model eccentric and precessing binaries with existing modelling frameworks, potentially allowing us to find eccentric and precessing binaries with detectors based on our models.

III. METHODS

We generate waveforms by the following three methods: (1) using pyEFPE [9] to generate eccentric-precessing inspiral waveforms from input parameters (2) using a PN code package [10] to generate dynamics of a system (such as spin and positions of black holes in orbit, parameterized by mean anomaly) in combination with code from Isaiah Tyler's previous SURF project to create the PN waveforms themselves and (3) using numerical relativity (NR) simulations from the Simulating Extreme Spacetimes (SXS) Catalog [11].

Using each waveform generation method, we will create a set of eccentric and precessing waveforms as well as a set of eccentric and non-precessing waveforms with the same mass, spin, and extrinsic parameters. We will then use the scri code package[12] to "untwist" the eccentric and precessing waveforms into the co-precessing frame.

By comparing each "untwisted" waveform to its eccentric non-precessing counterpart, both qualitatively and quantitatively, we can determine how well the transformation removes precession effects. Additionally, by comparing the efficacy of the transformation in removing pre-

cession between the three different waveform generation methods, we can evaluate each code package's accuracy as a model. In particular, since NR makes fewer approximations about the motion of binary objects, we can use comparison between the first two methods and the NR simulations to see if there is missing physics due to the approximations in the other two models.

IV. INTERIM RESULTS

We began by investigating changing different parameters to observe the resulting effects on GWs in the time domain. By plotting the effect of changing each parameter separately we could gain valuable intuition into the impact of individual parameters on a GW. The observations and plots from this parameter changing analysis are discussed in Section IV A. We have also begun to create and plot waveforms with two out of the three generation methods we will be using: the PN code (see Section IV B) and NR simulations from the SXS Catalog (see Section IV C).

A. Effect of Changing Parameters on Time-Domain Waveforms

We present our findings from changing five parameters in Table I. Each parameter has an associated figure depicting how it affects a waveform.

Parameter	Effect of Increasing Parameter
Total Mass (Figure 3)	Inspiral shortens and amplitude increases
Mass ratio (Figure 4)	Inspiral lengthens and amplitude decreases
z-axis spin (Figure 5)	Inspiral lengthens
Precession (Figure 6)	Amplitude modulates
Eccentricity (Figure 7)	Inspiral lengthens, amplitude (at periastron) increases, "knocking" effect (uneven amplitude per period)

TABLE I. Summary of Section IV A.

B. PN Model Waveforms

After exploring the effects of altering certain parameters, we experimented with the PN waveform generation method to learn how to use the code package and gain familiarity with the dynamics of eccentric and precessing waveforms. Though most of these figures are temporarily inaccessible due to a github merge problem, Figure 8 depicts the changing x,y, and z components of the orbital angular momentum in eccentric systems with varying amounts of precession. Our next step will be to use the eccprec code package from Isaiah Tyler's previous SURF project to turn these dynamics into time-domain strain waveforms.

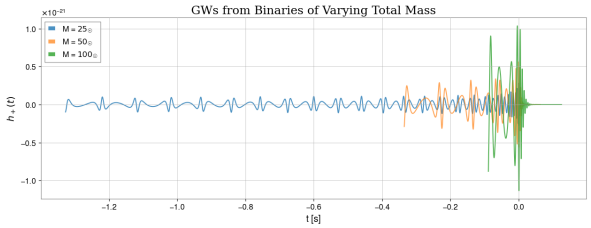

FIG. 3. Plus polarization of strain over time for GWs from eccentric binaries with varying total mass. The blue waveform is the longest and has the lowest total mass, while the green waveform is the shortest and has the highest total mass, indicating that increasing total mass shortens inspiral duration. Additionally, the strain amplitude of the waveform increases for higher mass systems.

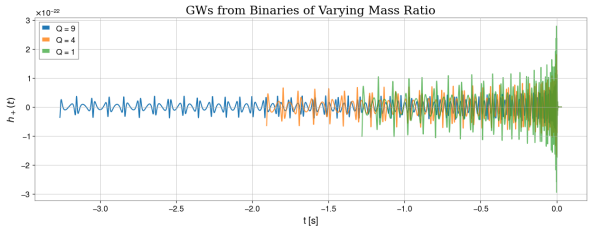

FIG. 4. Plus polarization of strain over time from eccentric BH binaries of varying mass ratio. The blue waveform is the longest and has the highest mass ratio (Q=9), while the green waveform is shortest and has an equal mass ratio. The waveforms with lower mass ratios also have higher amplitude strain. These qualities indicate that increasing mass ratio increases inspiral duration and decreases strain amplitude.

C. NR Waveforms

The SXS Catalog [11] has many examples of eccentric and precessing waveforms generated with NR. We have learned to use python to extract and plot the modes and strain of these waveforms.

V. CHALLENGES AND FUTURE STEPS

Our next steps will be to learn how to generate waveforms with pyEFPE and how to use the scri code package to untwist waveforms into the co-precessing frame. We will need to figure out how to format waveforms generated with our three previously described methods such that we can untwist them with the scri code, which we anticipate taking some time to work out. Before generating our large sets of eccentric and precessing waveforms, we will also need to characterize where in parameter space each of our three waveform generation methods retains accuracy.

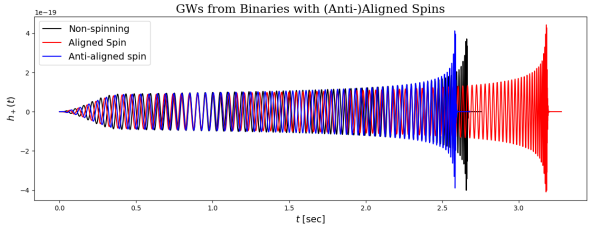

FIG. 5. Plus polarization of strain over time for anti-aligned spin (blue), non-spinning (black), and aligned spin (red) systems. The anti-aligned spin system has a shorter inspiral than the non-spinning system, while the aligned spin system is longer than the non-spinning system. This change of duration is due to the hang-up effect, wherein aligned spin adds to the amount of angular momentum the system needs to dissipate, increasing the time to merger, and vice versa for anti-aligned spin. The tapering in the first half-second of the inspiral is a feature of the LALSimulation code, not a physical effect.

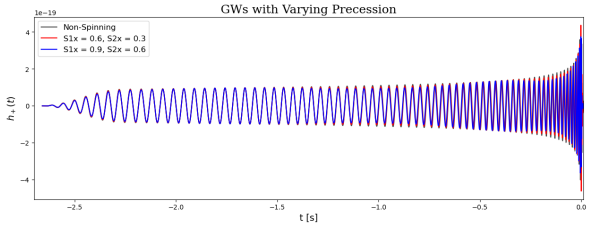

FIG. 6. Plus polarization of strain over time for BH binaries with varying amounts of precession. The black waveform is from a non-spinning system (which does not precess), the red waveform is from a precessing system, and the blue waveform is from a system with larger misaligned spin and thus more precession. The increase in severity of amplitude modulation as precession increases is clearly visible, particularly towards the end of the inspiral. As in Figure 5, the tapering at the start of the inspiral is a feature of the code, not a physical effect.

Once we have generated our sets of waveforms and untwisted the eccentric and precessing ones, we will need to determine the best evaluation metrics to quantitatively compare untwisted waveforms to their eccentric non-precessing counterparts. To do so, we anticipate needing to read some papers discussing evaluation metrics. Our initial ideas are to rely on a combination of qualitative comparisons between waveforms (such as those conducted in Section IV A), and **mismatches**. A mismatch is an inner product that reduces the difference between two waveforms to a single number ranging from 0 (orthogonal waveforms) to 1 (identical waveforms). Mismatches require a noise curve, which we will begin by setting to 1 (white noise), allowing us to assess intrinsic differences of the waveforms without reference to their detection.

[1] LIGO Scientific Collaboration, Virgo Collaboration, and KAGRA Collaboration, LVK Algorithm Library - LALSuite, Free software (GPL) (2018).

[2] M. Mapelli, Binary black hole mergers: Formation and populations, Frontiers in Astronomy and Space Sciences **7**, 10.3389/fspas.2020.00038 (2020).

[3] M. Favata, SXS, and K. Thorne, Elliptical binaries, Sounds of Spacetime (2025).

[4] T. A. Apostolatos, C. Cutler, G. J. Sussman, and K. S. Thorne, Spin-induced orbital precession and its modulation of the gravitational waveforms from merging binaries, Phys. Rev. D **49**, 6274 (1994).

[5] M. Favata, SXS, and K. Thorne, Spinning binaries, Sounds of Spacetime (2025).

[6] P. Schmidt, M. Hannam, and S. Husa, Towards models of gravitational waveforms from generic binaries: A simple approximate mapping between precessing and non-precessing inspiral signals, Phys. Rev. D **86**, 104063 (2012), arXiv:1207.3088 [gr-qc].

[7] M. Boyle, R. Owen, and H. P. Pfeiffer, Geometric approach to the precession of compact binaries, Physical Review D **84**, 10.1103/physrevd.84.124011 (2011).

[8] S. Albanesi, R. Gamba, S. Bernuzzi, J. Fontbuté, A. Gonzalez, and A. Nagar, Effective-one-body modeling for generic compact binaries with arbitrary orbits (2025), arXiv:2503.14580 [gr-qc].

[9] G. Morras, G. Pratten, and P. Schmidt, Improved post-Newtonian waveform model for inspiralling precessing-eccentric compact binaries, Phys. Rev. D **111**, 084052 (2025), arXiv:2502.03929 [gr-qc].

[10] K. S. Phukon, N. K. Johnson-McDaniel, A. Singh, and A. Gupta, Evolution of precessing binary black holes on eccentric orbits using orbit-averaged evolution equations, (2025), arXiv:2504.20543 [gr-qc].

[11] The sxs catalog of simulations (2025).

[12] M. Boyle, Angular velocity of gravitational radiation from precessing binaries and the corotating frame, Physical Review D **87**, 10.1103/physrevd.87.104006 (2013).

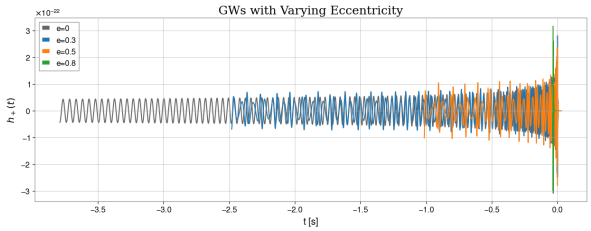

FIG. 7. Plus polarization of strain over time for BH binaries with varying eccentricity. The black waveform is from a circular binary, while the blue, orange, and green waveforms have increasing eccentricity. As the eccentricity approaches 1, the length of the inspiral decreases and the highest amplitude in each period increases. Additionally, the eccentric waveforms display the "knocking" effect described in Section I.

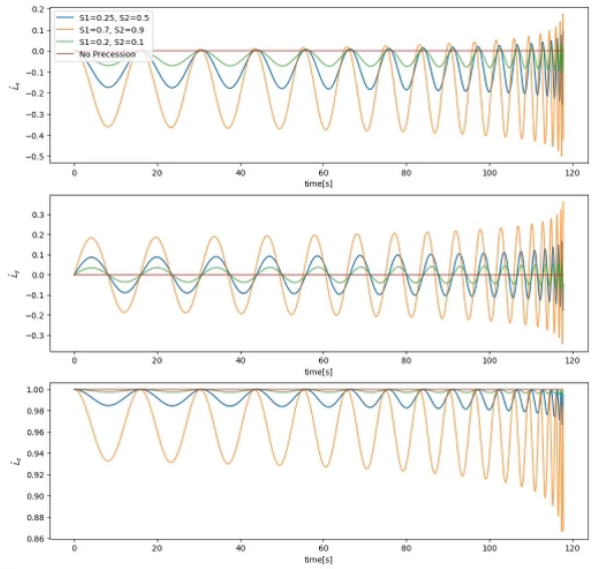

FIG. 8. Amplitude of x (top), y (middle), and z (bottom) components of orbital angular momentum unit vector ($\hat{L}$) over time during inspiral of eccentric binary with varying precession. The red line depicts $\hat{L}$ for a non precessing system, and the green, blue, and yellow lines depict systems with increasing amounts of precession from higher misaligned spins. The periodic fluctuation in each component of $\hat{L}$ depicts the precession cone traced out by the vector. This precession of $\hat{L}$ is highest amplitude for the yellow line, which is the system with the highest spin.